Pure appl. geophys. 158 (2001) 2227–2251
0033–4553/01/112227–25 $ 1.50 + 0.20/0

Pure and Applied Geophysics

Yield Estimation from Surface-wave Amplitudes

JEFFRY L. STEVENS[1] and JOHN R. MURPHY[1]

Abstract — Surface-wave amplitudes from explosion sources show less variation for a given event than body wave amplitudes, so it is natural to expect that yield estimates derived from surface waves will be more accurate than yield estimates derived from body waves. However, yield estimation from surface waves is complicated by the presence of tectonic strain release, which acts like one or more earthquake sources superimposed on top of the explosion. Moment-tensor inversion can be used to remove the tectonic component of the surface waves, however moment-tensor inversion for shallow sources is inherently non-unique so the explosion isotropic moment cannot be determined with the necessary accuracy by this means. Explosions on an island or near a mountain slope can exhibit anomalous surface waves similar to those caused by tectonic strain release. These complications cause yield estimates derived from surface waves to be less accurate than yield estimates from body waves recorded on a well-calibrated network with good coverage. Surface-wave amplitudes can be expressed as a surface-wave magnitude M_s, which is defined as the logarithm of the amplitude plus a distance correction, or as a path corrected spectral magnitude, log M_0', which is derived from the surface-wave spectrum. We derive relations for M_s vs. yield and log M_0' vs. yield for a large data set and estimate the accuracy of these estimates.

Key words: Surface wave, explosion, yield, magnitude, moment, moment tensor.

Introduction

The Threshold Test-Ban Treaty (TTBT) between the United States and the Soviet Union, which went into effect in 1976, limited the yield of underground nuclear tests to 150 kilotons. Because of this, accurate estimation of explosion yields from seismic data became very important, and a great deal of research was performed to identify all of the factors that caused variations in seismic amplitudes. This caused renewed interest in estimating explosion yields from surface waves. These yield estimates were then used as a consistency check on other phases, or combined with the other estimates to obtain a unified yield (RINGDAL *et al.*, 1992; MURPHY, 1993) using all measurements at the same time.

Surface waves have some advantages and disadvantages for yield estimation compared to other phases. Surface-wave amplitudes exhibit less scatter than other phases, with a network standard deviation in M_s typically about half the standard deviation for m_b (BACHE, 1982). Also, since surface waves are usually measured at periods of about 20 seconds, they are much less sensitive to small-scale variations in

[1] Science Applications International Corporation. E-mail: Jeffry.L.Stevens@saic.com

the earth than short-period regional and teleseismic phases. Since the measured period is considerably longer than the explosion source duration, this also means that surface waves are insensitive to the explosion source function. That is, while surface-wave amplitudes will vary in different materials with source coupling, they are not affected by details of the source spectrum which are flat at periods longer than a few seconds. On the negative side, surface waves cannot be measured to as small a magnitude as m_b. This is particularly true for explosions where m_b is 1–2 magnitude units higher than M_s. Also, while surface waves are less sensitive to variations in attenuation and scatter than m_b, they are subject to variations due to tectonic strain release and near-source structure that have little effect on m_b. The sources and magnitude of these variations are discussed later in this paper.

Because surface waves are long-period measurements, surface-wave amplitudes are approximately proportional to explosion yield, and the slope of the magnitude yield curve is close to one. That is, we can write $M_s = \log Y + C$, where Y is the yield in kilotons (KT) and C is a constant that may depend on source medium, but is independent of explosion yield. For example, BACHE (1982) using data from MARSHALL *et al.* (1979), found $M_s = \log Y + 2.05 \pm 0.21$. There are a number of other similar relations in the literature. MURPHY (1977) found $M_s = 0.84 \log Y + 2.14$ and $M_s = 1.33 \log Y + 1.20$ for explosions with yield less than and greater than 100 kilotons, respectively. MARSHALL *et al.* (1979) found $M_s = 0.97 \log Y + 2.16$ for explosions in salt and granite, and $M_s = 1.06 \log Y + 1.88$ for all explosions in their data set including poorly coupling events above the water table. In general, however, these relations have been derived as best fits to data including events in different materials with varying depths, and are also consistent with unit slope for explosions in similar materials at comparable depth.

Since an idealized explosion is spherically symmetric, and when embedded in a plane layered structure is cylindrically symmetric, such an explosion should generate no Love waves and should generate Rayleigh waves with the same amplitude in all directions. It is well known, however, that explosions generate Love waves, which can be quite large in some cases, and that the Rayleigh waves not only have a radiation pattern, but can be reversed, as if from an implosive source, in some cases (e.g., TOKSÖZ and KEHRER, 1972). Figure 1 shows an example of Rayleigh and Love waves recorded at the same station for two explosions at the Soviet Semipalatinsk test site. The first set of seismograms shows a normal Rayleigh wave and a small Love wave; the second shows a reversed Rayleigh wave and a Love wave comparable in amplitude to the Rayleigh wave. This anomalous radiation can be explained by superposition of one or more earthquake-like sources on top of the explosion source. Explanations for this extra source include tectonic strain release (ARCHAMBEAU, 1972; STEVENS, 1982; DAY *et al.* 1987; HARKRIDER *et al.*, 1994), earthquake triggering (AKI and TSAI, 1972), and passive block motion (SALVADO and MINSTER, 1980; MASSE, 1981). VIECELLI (1973) suggested that spall could be a strong generator of surface waves, and a possible mechanism for reversed Rayleigh waves. However

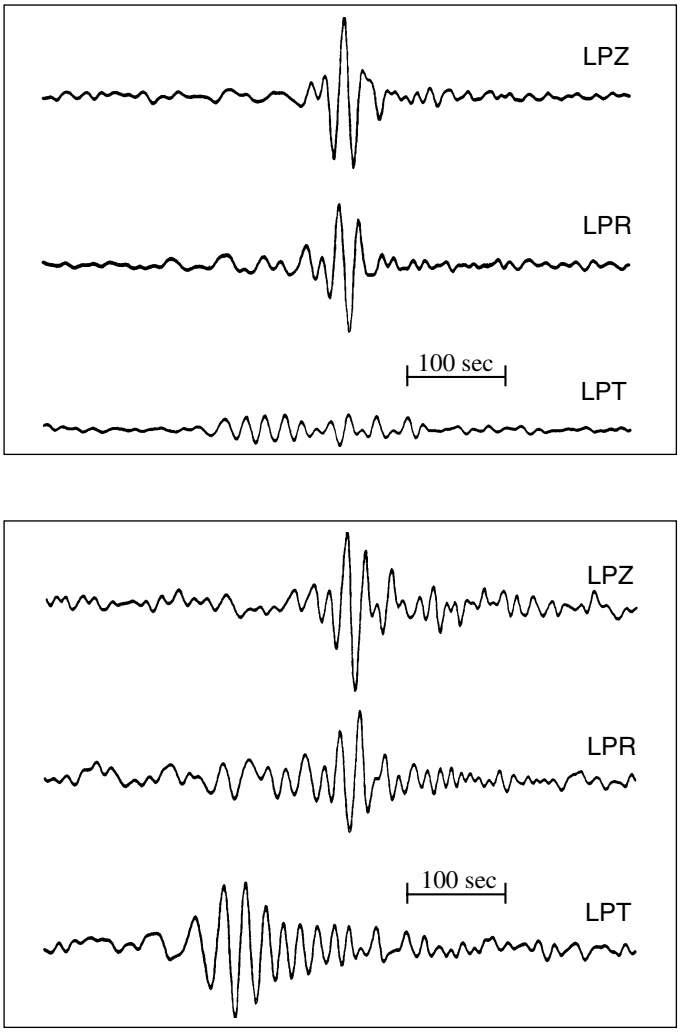

Figure 1
Long-period vertical, radial, and transverse components of displacement recorded at the same station from two explosions at the Semipalatinsk test site. The first event (top) has a normal Rayleigh wave and a small Love wave on the transverse component. The seismogram from the second event (bottom) shows a Love wave comparable in amplitude to the Rayleigh wave, and the Rayleigh wave phase shifted, approximately reversed, with respect to the normal Rayleigh wave.

DAY *et al.* (1983), showed conclusively that spall cannot contribute significantly to surface waves at periods longer than a few seconds. An initially puzzling aspect of the observations of Rayleigh wave reversals was an apparent time delay of the anomalous Rayleigh waves compared to normal Rayleigh waves from nearby locations (RYGG, 1979; HELLE and RYGG, 1984; HERRIN and GOFORTH, 1986). However, this time delay proved to be easily explained by interference between the

explosion and double-couple source functions (DAY and STEVENS, 1986; DAY *et al.*, 1987; STEVENS *et al.*, 1991).

All of the feasible mechanisms for explaining the anomalous surface waves have the characteristic that they can be described at the periods of interest (greater than about 10 seconds) by superposition of one or more double-couple sources, or an equivalent moment-tensor source, on top of a point explosion source. Moment-tensor inversion has been used to separate the isotropic and nonisotropic parts of the source so that the explosion yield could be determined from the isotropic source alone. A fundamental problem with moment-tensor inversion for shallow sources is that the solution is non-unique and some additional constraint is required. GIVEN and MELLMAN (1986) performed moment-tensor inversions for 37 Shagan River (Russia) explosions and 47 Nevada Test Site (NTS) explosions. They constrained the Shagan River explosions to a 45 degree thrust mechanism, and the NTS explosions to a strike-slip mechanism, and the inversion then determined the strike of the double-couple source and the isotropic and double-couple moments for each event. They determined these constraints by plotting the function $0.9 \log M_i - m_b$ as a function of F factor (the ratio of nonisotropic to isotropic moment) for the isotropic moment M_i derived for different source constraints, and finding the source constraint that minimized the slope of this function. The assumption here is that isotropic moment is proportional to yield Y and m_b is proportional to $0.9 \log Y$ so that the difference $0.9 \log M_i - m_b$ should be constant if the constraint is correct and consistent for a test site. It is important to recognize, however, that selecting different mechanisms for the two test sites creates a very significant bias in the results as the thrust fault assumption increases M_i relative to the strike-slip assumption.

EKSTRÖM and RICHARDS (1994) found that the constraint of a constant mechanism at each site was too strong and led to unrealistic results in some cases. They used announced yields, and yields derived from m_b and Lg as additional constraints and performed moment-tensor inversions on a larger set of Shagan River explosions, and were then able to determine both the dip-slip and strike-slip components. They found solutions more consistent with Shagan River geology, and determined a moment yield relation of $\log M_i = \log Y + 14.31$ where Y is yield in kilotons and M_i is isotropic moment in Newton-meters. However, they also found that because of the variability in the source mechanism they were unable to determine isotropic moments that gave satisfactory results without detailed knowledge about each explosion.

An assumption used in most moment-tensor inversions is that the nonisotropic source can be described by a single double-couple source. However, this is not necessarily the case. DAY *et al.* (1987), for example, performed axisymmetric calculations of an explosion in a uniformly prestressed medium and showed that Rayleigh wave reversals could be obtained with shear stress levels of 100 bars or greater. Uniformly prestressed means that the M_{xx} and M_{yy} moment-tensor components are equal. This source produces reduced or reversed Rayleigh waves,

but no Love waves, making moment-tensor inversion for the isotropic source even more difficult to accomplish.

In addition to problems with tectonic release, STEVENS *et al.* (1993) found that a long-period amplitude reduction can occur if the explosion is on an island or near a mountain slope. If there is a free surface such as a cliff or a sharp mountain boundary, it allows stress to be relaxed in the horizontal direction, leading to a reduction in the amplitude of generated surface waves. This happens because the distortion caused by the explosion goes into a permanent displacement of the slope rather than being radiated away by surface waves. This effect appears to have been a contributor to anomalous surface waves from Novaya Zemlya explosions.

Surface-wave Magnitudes

Yield estimates derived from surface waves are calculated by measuring a surface-wave magnitude and then using a magnitude yield relation to estimate the yield. "Magnitude" is used in a generalized sense here to mean a set of surface-wave measurements with corrections applied to give a measure of source strength, and therefore includes isotropic moment derived from moment-tensor inversion as well as time domain and spectral magnitudes. We consider three types of magnitudes: time domain M_s, path-corrected spectral magnitude $\log M_0'$, and isotropic moment M_i. We also compare results for network-averaged and maximum likelihood magnitudes.

The surface-wave magnitude M_s corrects for distance and is a measure of the size of the source, or more accurately, the part of the source that generates surface waves. The IASPEI formula for M_s is given by

$$M_s = \log \frac{A}{T} + 1.66 \log \Delta + 0.3 \ , \tag{1}$$

where A is the zero-to-peak amplitude in nanometers, Δ is the distance in degrees and T is the measured period in seconds. M_s magnitudes reported by the U.S. Geological Survey (USGS) are made on the vertical component and are measured between periods of 18 and 22 seconds. A problem with the IASPEI formula is that the distance correction becomes increasingly inaccurate at short distances. An improved M_s formula with better distance independence was derived by REZAPOUR and PEARCE (1998) and is based on the theoretical functional form for propagating surface waves (SATO, 1967), with constant factors derived using the entire ISC M_s data set:

$$M_s = \log \frac{A}{T} + \frac{1}{3}\log(\Delta) + \frac{1}{2}\log(\sin(\Delta)) + 0.0046\Delta + 2.370 \ . \tag{2}$$

The $1/3 \log(\Delta)$ term is an Airy phase approximation for the effect of time domain dispersion. This formula has recently been adopted by the International Data Center (IDC), replacing the IASPEI M_s formula.

The path-corrected spectral magnitude $\log M_0'$ is defined as the logarithm of the spectral amplitude divided by the Green's function for an explosion-generated surface wave for the source to receiver path:

$$M_0' = \left| u_z(\omega, r, \theta) \Big/ \frac{S_1^x(\omega, h_x) S_2(\omega) \exp[-\gamma_p(\omega) r + i(\varphi_0 - \omega r / c_p(\omega))]}{\sqrt{a_e \sin(r/a_e)}} \right| , \qquad (3)$$

where u_z is the measured spectral amplitude on the vertical component, S_1^x is a function that depends on the properties of the source region, S_2 is a function that depends on the receiver region, r is the source to receiver distance, a_e is the radius of the earth, and c_p and γ_p are the phase velocity and attenuation coefficients averaged over the source-to-receiver path. Definitions of the functions are given in Appendix A. For an explosion source with no tectonic release, $M_0' = 3\frac{\beta^2}{\alpha^2} M_i$ where M_i is the explosion isotropic moment. M_0' is defined this way so that the source region excitation function is not explicitly dependent on local material properties at shallow source depths. The functional form of the path-corrected spectral magnitude is similar to the Rezapour and Pearce magnitude, equation (2), except for omission of the Airy phase dispersion correction which is not needed in the frequency domain. Equation (3) has the advantage that it can be regionalized, calculating the earth structure dependent quantities using different structures in different regions. STEVENS and MCLAUGHLIN (2001) discuss this in more detail.

Moment-tensor inversion is a technique for determining the explosion isotropic moment M_i by removing the contaminating nonisotropic source which generates surface waves that are superimposed on top of the explosion-generated surface waves. Although moment-tensor inversion is widely used in earthquake studies, explosions are a special case because the solution becomes nonunique for shallow sources. Details of the techniques for moment-tensor inversion for shallow explosion sources are given by GIVEN and MELLMAN (1986) and EKSTRÖM and RICHARDS (1994), and are summarized in Appendix A. In brief, moment-tensor inversion requires an additional constraint on the nonisotropic source, and this constraint has a very significant effect on the solution. The constraint usually takes the form of assuming that the nonisotropic source can be described by a double-couple source, and then fixing the strike, dip, or rake, or some combination of these parameters. The magnitude of the error that can result from the incorrect choice of this constraint is shown in Figure 2. This figure shows the error in log isotropic moment that results when tectonic release of general rake λ and dip δ are interpreted under the assumption that the tectonic release corresponds to a strike-slip mechanism. The error in moment was calculated for $F = 0.3$, where F is the ratio of double-couple to isotropic moment, and is as large as ± 0.2 magnitude units.

The isotropic moment inferred from moment-tensor inversion will be equal to the average path-corrected spectral magnitude (log of equation (3)) plus a term that depends on the magnitude and orientation of the nonisotropic source. A strike-slip

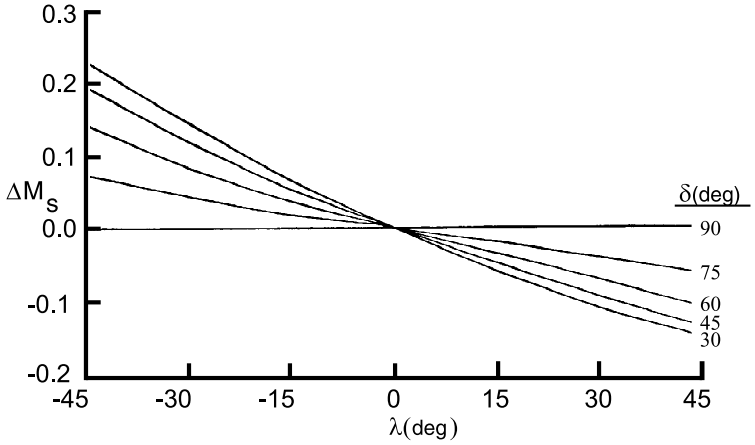

Figure 2
Error in log isotropic moment (labeled ΔM_s) for an event with $F = 0.3$ as a function of rake, for several values of dip, when the tectonic release is interpreted under a strike-slip assumption (rake $\lambda = 0°$, dip $\delta = 90°$). F is the ratio of double-couple to isotropic moment.

constraint has a minimal effect on the result, because the nonisotropic source increases the surface waves over a 180 degree range and decreases the surface waves over a 180 degree range, so if coverage is good, then the isotropic moment will be very close to the average value of the path-corrected spectral magnitudes. A 45-degree dip-slip (thrust) mechanism, on the other hand, decreases the surface-wave amplitudes at all azimuths, so moment-tensor inversion with this constraint increases the isotropic moment. Conversely, a normal fault increases the surface-wave amplitudes at all azimuths, so moment-tensor inversion with this constraint decreases the isotropic moment. A vertical dip-slip mechanism is never used as a constraint because this source generates very small surface waves at shallow depths. A more complicated situation is a complex linear vector dipole (CLVD) source, which is equivalent to two 45-degree thrust faults at right angles to each other. The CLVD source is cylindrically symmetric and therefore generates no Love waves and no azimuthal variations in Rayleigh waves. Consequently, it cannot be removed by moment-tensor inversion, but it can affect the surface-wave amplitudes as strongly as a thrust mechanism.

Surface-wave Magnitude Measurements

Surface-wave magnitudes, M_s and path-corrected spectral magnitudes $\log M_0'$ were measured from a large historical data set of surface waves from underground nuclear tests. M_s measurements were made using the techniques now in the operational system at the International Data Center (see STEVENS and MCLAUGHLIN, 2001), and using the Rezapour and Pearce definition of M_s. Noise levels were measured for all waveforms where a surface wave could not be identified. These noise

levels were used as upper bounds for calculation of maximum likelihood (MLE) magnitudes, and maximum likelihood magnitudes and station corrections were derived for all events. Table 1 lists the events, network-averaged and MLE magnitudes, and known or estimated yields for each event. The purpose of maximum likelihood magnitudes is to compensate for the bias that results when lower amplitude measurements are lost in noise and only higher amplitude measurements are used. However, MLE magnitudes tend to be smaller than network-averaged magnitudes even for well-recorded events, so we treat them here as separate magnitude measures.

Table 1 also lists isotropic moments from the moment-tensor inversion results of GIVEN and MELLMAN (1986). EKSTRÖM and RICHARDS (1994) give a more extensive list of moment-tensor inversion results for the Shagan River test site, however their moments were normalized to moments derived from regional phases, and are therefore somewhat higher than the Given and Mellman moments, which were derived using the surface-wave path corrections of STEVENS (1986).

Magnitude Yield Relations

Yields have been released for only a few of the events listed in Table 1. The yields for U.S. tests are from DOE (1994), and for Russian tests from MIKHAILOV (1996). Yields for the three Amchitka explosions and for Handley are approximate. The three earliest Shagan River explosions have announced yields. We have also included estimated yields derived from m_b and m_bLg measurements as derived by RINGDAL *et al.* (1992) for the remaining Shagan River explosions. For each magnitude type, we have derived a linear data fit with slope 1 of the form:

$$M = \log Y + C \quad . \tag{4}$$

Table 2 lists the value and standard deviation of the constant C for each magnitude for all events with known yields, and for each test site. Figures 3–7 show the different magnitudes plotted vs. yield for all of the data.

Figure 8 shows the difference between log isotropic moment and log yield plotted as a function of F factor for all of the events with both isotropic moments and yields or yield estimates. The scatter is comparable to or greater than the uncertainty due to the variation in source mechanism shown in Figure 2.

We can also compare the moment estimates with theoretical and empirical models of explosion source functions. The Mueller Murphy source model (MUELLER and MURPHY, 1971; MURPHY and MUELLER, 1971) is an empirical fit to the explosion source function that was derived from near-field records of explosions in a variety of materials. Depth dependence is included explicitly in the Mueller Murphy source, and for explosions at standard containment depth ($\sim$122 m/kt$^{1/3}$) this model predicts moment proportional to $Y^{0.76}$. We also compare with two numerical models of explosions in tuff, salt and granite (STEVENS and DAY, 1985). These calculations were

Table 1

Surface-wave magnitude measurements for 207 nuclear explosions

Testsite	Date	Event Name	m_b	M_s Ave	M_s MLE	Stdev	Log M_0' Ave	Log M_0' MLE	Stdev	Nsig	Nnoise	Log M_i	Yield
AHAGGAR	1963293	rubis	5.62	4.26	4.16	0.25	16.18	16.00	0.22	2	0		52
AHAGGAR	1965058	saphir	5.88	4.64	4.60	0.16	16.43	16.35	0.16	3	0		120
AMCHITKA	1965302	longshot	6.03	3.95	3.76	0.12	15.62	15.44	0.06	8	5		80
AMCHITKA	1969275	milrow	6.52	5.00	4.94	0.06	16.56	16.49	0.06	23	3		≈ 1000
AMCHITKA	1971310	cannikin	6.89	5.70	5.68	0.07	17.31	17.26	0.06	26	2		< 5000
CLIMAX	1966153	piledriver	5.56	3.99	3.99	0.14	15.97	15.86	0.06	10	1		62
DEGELEN	1967057	deg26feb67	6.00	3.80	3.64	0.25	15.85	15.74	0.01	2	0		
DEGELEN	1972345	deg10dec72	5.60	4.42	4.39	0.07	16.14	16.07	0.05	7	0		
DEGELEN	1977302	deg29oct77	5.60	3.96	3.74	0.11	15.75	15.47	0.09	4	4		
DEGELEN	1978085	deg26mar78	5.61	4.07	3.61	0.10	15.92	15.45	0.09	3	6		
DEGELEN	1978112	deg22apr78	5.28	3.36	3.17	0.04	15.40	15.06	0.08	3	5		
DEGELEN	1978209	deg28jul78	5.66	3.36	3.15	0.04	15.32	15.01	0.04	2	6		
DEGELEN	1979151	deg31may79	5.24	3.35	3.04	0.11	15.21	14.83	0.07	2	9		
DEGELEN	1980143	deg22may80	5.49	3.26	3.12	0.10	15.10	14.92	0.07	4	8		
DEGELEN	1980213	deg31jul80	5.30	3.70	3.56	0.13	15.50	15.35	0.09	5	6		
DEGELEN	1987157	deg06jun87	5.30	2.07	2.02	0.25	14.66	14.52	0.04	2	24		
DEGELEN	1987198	deg17jul87	5.80	3.77	3.33	0.22	15.73	15.33	0.30	4	17		
LOPNOR	1996160	lop08jun96	5.69	4.05	4.03	0.09	15.72	15.75	0.04	4	1		
MURUROA	1977078	mur19mar77	5.73	4.13	4.04	0.16	15.91	15.88	0.18	3	2		
MURUROA	1977328	mur24nov77	5.80	4.16	3.95	0.10	15.77	15.67	0.20	3	3		
MURUROA	1978334	mur30nov78	5.80	4.37	3.96	0.17	15.86	15.62	0.08	4	5		
MURUROA	1979206	mur25jul79	6.03	4.05	3.94	0.04	15.79	15.65	0.13	5	3		
MURUROA	1980338	mur03dec80	5.58	3.84	3.52	0.12	15.59	15.24	0.08	2	7		
MURUROA	1982206	mur25jul82	5.60	3.88	3.79	0.06	15.61	15.54	0.08	6	8		
MURUROA	1983109	mur19apr83	5.60	4.05	3.94	0.08	15.86	15.75	0.10	8	8		
MURUROA	1983145	mur25may83	5.90	3.97	3.82	0.08	15.74	15.64	0.11	8	7		
MURUROA	1984133	mur12may84	5.70	3.87	3.56	0.10	15.61	15.37	0.13	4	11		
MURUROA	1984307	mur02nov84	5.70	4.23	3.71	0.11	15.93	15.47	0.11	2	12		
MURUROA	1984341	mur06dec84	5.60	3.99	3.80	0.11	15.68	15.50	0.10	7	5		
MURUROA	1985330	mur26nov85	5.80	4.04	3.95	0.06	15.93	15.65	0.18	5	10		
MURUROA	1987140	mur20may87	5.60	3.89	3.64	0.09	15.52	15.34	0.07	4	7		

Table 1

continued

Testsite	Date	Event Name	m_b	M_s Ave	M_s MLE	Stdev	Log M_0' Ave	Log M_0' MLE	Stdev	Nsig	Nnoise	Log M_i	Yield
NN_ZEMLYA	1967294	nnz21oct67	5.99	3.82	3.69	0.19	15.49	15.33	0.07	7	6		
NN_ZEMLYA	1968312	nnz07nov68	6.11	4.17	4.09	0.22	16.06	15.97	0.13	8	0		
NN_ZEMLYA	1970287	nnz14oct70	6.77	5.00	4.94	0.07	16.56	16.49	0.05	28	4		
NN_ZEMLYA	1973255	nnz12sep73	6.96	5.37	5.29	0.10	16.88	16.77	0.11	10	3		
NN_ZEMLYA	1974241	nnz29aug74	6.54	4.94	4.87	0.08	16.54	16.43	0.05	24	2		
NN_ZEMLYA	1975235	nnz23aug75	6.55	4.85	4.76	0.10	16.27	16.14	0.09	18	4		
NN_ZEMLYA	1976273	nnz29sep76	5.77	3.63	3.41	0.14	15.34	15.10	0.07	6	2		
NN_ZEMLYA	1976294	nnz20oct76	4.89	3.40	3.25	0.01	15.02	14.72	0.04	2	2		
NN_ZEMLYA	1977244	nnz01sep77	5.71	4.22	4.27	0.17	15.40	15.33	0.12	5	0		
NN_ZEMLYA	1978222	nnz10aug78	6.04	3.94	3.64	0.08	15.54	15.13	0.07	6	9		
NN_ZEMLYA	1978270	nnz27sep78	5.68	4.16	4.09	0.05	15.80	15.74	0.06	9	1		
NN_ZEMLYA	1979267	nnz24sep79	5.80	4.24	4.14	0.07	15.75	15.63	0.06	7	2		
NN_ZEMLYA	1979291	nnz18oct79	5.85	4.21	3.79	0.13	15.37	15.05	0.06	2	7		
NN_ZEMLYA	1980285	nnz11oct80	5.80	3.89	3.76	0.11	15.52	15.36	0.06	7	6		
NN_ZEMLYA	1981274	nnz01oct81	5.91	4.13	4.10	0.09	15.75	15.67	0.07	9	4		
NN_ZEMLYA	1982284	nnz11oct82	5.52	3.82	3.66	0.13	15.38	15.22	0.06	9	6		
NN_ZEMLYA	1983230	nnz18aug83	5.84	3.97	3.86	0.05	15.65	15.54	0.10	2	16		
NN_ZEMLYA	1983268	nnz25sep83	5.71	3.82	3.52	0.09	15.31	15.10	0.08	6	12		
NN_ZEMLYA	1984299	nnz25oct84	5.80	3.99	3.92	0.06	15.76	15.65	0.06	10	6		
NN_ZEMLYA	1987214	nnz02aug87	5.80	3.93	3.81	0.09	15.61	15.42	0.08	11	11		
NN_ZEMLYA	1988128	nnz07may88	5.60	4.01	3.89	0.08	15.51	15.45	0.05	14	4		
NN_ZEMLYA	1988339	nnz04dec88	5.90	4.06	3.93	0.08	15.71	15.59	0.05	12	4		
NN_ZEMLYA	1990297	nnz24oct90	5.40	3.99	3.86	0.08	15.61	15.44	0.10	14	5		
PAHUTE	1966181	halfbeak	6.10	4.70	4.58	0.25	16.70	16.49	0.06	2	0		365
PAHUTE	1967143	scotch	5.70	4.55	4.50	0.08	16.47	16.34	0.07	12	1	16.46	155
PAHUTE	1968082	stinger	5.60	4.23	4.14	0.10	16.15	16.04	0.04	10	2		
PAHUTE	1968117	boxcar	6.30	5.36	5.32	0.06	17.07	16.94	0.10	11	2		1300
PAHUTE	1968242	sled	5.90	4.28	4.23	0.09	16.19	16.11	0.04	12	2		
PAHUTE	1968354	benham	6.30	5.47	5.35	0.07	17.10	16.95	0.07	8	3		1150
PAHUTE	1969127	purse	5.80	4.48	4.43	0.07	16.34	16.24	0.04	18	1		
PAHUTE	1970085	handley	6.50	5.26	5.22	0.06	16.94	16.80	0.07	9	3		> 1000

PAHUTE	1973157	almendro	6.10	4.88	4.72	0.08	16.59	16.49	0.07	11	4		
PAHUTE	1975134	tybo	6.00	4.71	4.61	0.06	16.49	16.42	0.03	11	4		
PAHUTE	1975154	stilton	5.90	4.26	4.18	0.07	16.23	16.09	0.07	10	3		
PAHUTE	1975170	mast	6.10	4.71	4.55	0.09	16.50	16.39	0.06	10	2		
PAHUTE	1976045	cheshire	6.00	4.87	4.68	0.13	16.67	16.47	0.06	11	5		
PAHUTE	1976069	estuary	6.00	4.93	4.67	0.10	16.61	16.41	0.04	5	2		
PAHUTE	1976077	pool	6.10	4.56	4.45	0.08	16.38	16.20	0.04	7	2		
PAHUTE	1978101	backbeach	5.50	4.14	3.92	0.08	16.05	15.76	0.09	4	6		
PAHUTE	1978243	panir	5.60	4.00	3.93	0.09	15.86	15.74	0.07	13	3		
PAHUTE	1978350	farm	5.50	4.17	4.07	0.07	15.94	15.79	0.08	8	4		
PAHUTE	1979162	pepato	5.50	4.15	4.10	0.06	16.08	16.03	0.04	22	2		
PAHUTE	1979269	sheepshead	5.60	4.07	4.01	0.06	15.95	15.86	0.03	17	4		
PAHUTE	1980117	colwick	5.40	4.00	3.93	0.11	15.90	15.79	0.06	7	2		
PAHUTE	1980164	kash	5.60	4.24	4.11	0.06	16.11	15.97	0.06	16	8		
PAHUTE	1980207	tafi	5.50	4.29	4.20	0.05	16.11	16.01	0.04	15	3		
PAHUTE	1981157	harzer	5.50	4.00	3.62	0.17	15.60	15.48	0.07	4	3		
PAHUTE	1987108	delamar	5.50	4.06	3.97	0.05	15.89	15.62	0.09	8	6		
PAHUTE	1987120	hardin	5.50	4.08	3.95	0.11	16.08	15.76	0.16	9	12		
PAHUTE	1987267	lockney	5.70	4.22	4.15	0.06	16.01	15.95	0.05	13	1		
PAHUTE	1988230	kearsarge	5.50	4.05	3.87	0.08	15.85	15.61	0.10	7	9		
SHAGAN	1969334	sha30nov69	6.00	3.78	3.68	0.08	15.89	15.74	0.07	4	2		125
SHAGAN	1972307	sha02nov72	6.14	3.87	3.80	0.09	15.73	15.64	0.07	11	1		165
SHAGAN	1972345	sha10dec72	6.00	4.42	4.39	0.07	16.14	16.07	0.06	7	0		140
SHAGAN	1973204	sha23jul73	6.18	4.12	4.07	0.08	15.85	15.71	0.05	10	2		212
SHAGAN	1973348	sha14dec73	5.82	3.82	3.76	0.10	15.95	15.88	0.04	5	0		80
SHAGAN	1976186	sha04jul76	5.81	3.80	3.82	0.12	15.67	15.65	0.15	5	0		65
SHAGAN	1976342	sha07dec76	5.90	4.11	3.84	0.08	15.72	15.39	0.13	2	2		54
SHAGAN	1977149	sha29may77	5.77	3.26	3.11	0.25	15.39	15.16	0.01	2	2		44
SHAGAN	1977180	sha29jun77	5.22	3.16	3.01	0.25	14.96	14.74	0.22	2	2		9
SHAGAN	1977248	sha05sep77	5.74	3.90	3.81	0.06	15.59	15.50	0.09	4	2		78
SHAGAN	1977302	sha29oct77	5.54	3.97	3.74	0.10	15.76	15.47	0.09	4	4		50
SHAGAN	1978162	sha11jun78	5.86	4.16	4.11	0.10	15.93	15.86	0.06	11	1		58
SHAGAN	1978186	sha05jul78	5.83	3.53	3.39	0.12	15.33	15.11	0.10	4	4		57
SHAGAN	1978241	sha29aug78	5.95	3.65	3.48	0.12	15.59	15.44	0.06	5	4	15.91	119

Table 1

continued

Testsite	Date	Event Name	m_b	M_s Ave	M_s MLE	Stdev	Log M_0' Ave	Log M_0' MLE	Stdev	Nsig	Nnoise	Log M_i	Yield
SHAGAN	1978258	sha15sep78	5.99	4.00	3.83	0.09	15.75	15.62	0.07	7	3	16.05	81
SHAGAN	1978308	sha04nov78	5.56	3.82	3.65	0.13	15.45	15.30	0.05	5	2	15.94	44
SHAGAN	1978333	sha29nov78	6.07	3.98	3.88	0.05	15.73	15.64	0.03	7	1	16.08	101
SHAGAN	1979032	sha01feb79	5.38	2.74	2.73	0.03	14.97	14.67	0.05	2	7		18
SHAGAN	1979174	sha23jun79	6.22	3.97	3.82	0.10	15.78	15.68	0.05	7	3	16.25	149
SHAGAN	1979188	sha07jul79	5.83	4.25	3.77	0.21	16.16	15.67	0.19	3	7	15.88	97
SHAGAN	1979216	sha04aug79	6.16	4.11	4.02	0.05	15.92	15.84	0.05	11	4	16.27	153
SHAGAN	1979230	sha18aug79	6.12	3.92	3.74	0.08	15.69	15.49	0.12	7	4	16.02	179
SHAGAN	1979301	sha28oct79	5.96	4.12	4.03	0.05	15.88	15.82	0.04	13	3	16.29	139
SHAGAN	1979336	sha02dec79	6.01	4.18	4.11	0.04	16.01	15.94	0.04	8	3	16.14	93
SHAGAN	1979357	sha23dec79	6.18	3.93	3.77	0.06	15.59	15.44	0.06	10	7	15.90	137
SHAGAN	1980164	sha12jun80	5.59	3.35	3.08	0.09	15.17	14.91	0.05	3	8	15.46	37
SHAGAN	1980181	sha29jun80	5.74	3.49	3.35	0.09	15.28	15.11	0.12	5	7	15.61	44
SHAGAN	1980258	sha14sep80	6.21	4.06	3.94	0.07	15.80	15.71	0.06	9	3	16.33	196
SHAGAN	1980286	sha12oct80	5.90	4.03	3.94	0.06	15.89	15.80	0.03	9	5	16.19	102
SHAGAN	1980349	sha14dec80	5.95	3.90	3.85	0.06	15.65	15.61	0.09	10	4	16.10	101
SHAGAN	1980362	sha27dec80	5.88	3.94	3.58	0.13	15.78	15.35	0.11	4	8	15.45	100
SHAGAN	1981088	sha29mar81	5.61	3.55	3.37	0.04	15.30	15.12	0.06	5	7	15.74	30
SHAGAN	1981112	sha22apr81	6.05	4.08	4.03	0.04	15.88	15.87	0.03	9	1	16.11	92
SHAGAN	1981147	sha27may81	5.46	3.16	2.79	0.07	14.86	14.70	0.04	2	8		20
SHAGAN	1981256	sha13sep81	6.18	4.06	4.01	0.06	15.94	15.90	0.06	5	1	16.26	163
SHAGAN	1981291	sha18oct81	6.11	4.19	4.10	0.04	15.94	15.87	0.05	6	8	16.16	107
SHAGAN	1981361	sha27dec81	6.31	4.31	4.17	0.09	15.96	15.86	0.04	9	6	16.19	156
SHAGAN	1982115	sha25apr82	6.10	4.10	3.96	0.03	15.83	15.68	0.04	7	8	16.17	145
SHAGAN	1982339	sha05dec82	6.10	4.16	4.00	0.07	15.94	15.76	0.04	9	6	16.19	119
SHAGAN	1983163	sha12jun83	6.10	4.39	4.27	0.04	16.15	16.04	0.04	12	7	16.30	138
SHAGAN	1983279	sha06oct83	6.00	4.21	4.15	0.07	16.06	15.95	0.05	11	5	16.27	82
SHAGAN	1983299	sha26oct83	6.10	4.25	4.11	0.06	15.98	15.80	0.06	7	9	16.33	114
SHAGAN	1984050	sha19feb84	5.80	4.21	4.08	0.06	15.91	15.79	0.05	8	6	15.98	49
SHAGAN	1984089	sha29mar84	5.90	4.12	3.88	0.08	15.85	15.71	0.04	6	9	16.04	83
SHAGAN	1984116	sha25apr84	5.90	4.35	4.11	0.05	16.17	15.93	0.09	6	7	16.18	76

SHAGAN	1984196	sha14jul84	6.20	4.33	4.28	0.05	16.13	16.06	0.06	14	2	16.28	135
SHAGAN	1984301	sha27oct84	6.20	4.29	4.14	0.08	15.99	15.84	0.06	13	6	16.24	165
SHAGAN	1984337	sha02dec84	5.80	4.08	3.92	0.12	15.80	15.64	0.08	11	7	16.11	79
SHAGAN	1984351	sha16dec84	6.10	4.28	4.17	0.07	16.11	16.01	0.05	14	6	16.36	137
SHAGAN	1984363	sha28dec84	6.00	4.15	4.06	0.05	15.84	15.76	0.05	11	7	15.90	105
SHAGAN	1985041	sha10feb85	5.90	4.26	4.15	0.06	16.07	15.94	0.05	11	5	16.21	62
SHAGAN	1985115	sha25apr85	5.90	4.04	3.75	0.13	15.85	15.55	0.11	8	10		74
SHAGAN	1985166	sha15jun85	6.00	4.00	3.90	0.06	15.71	15.65	0.03	13	5		114
SHAGAN	1985181	sha30jun85	6.00	4.06	3.92	0.05	15.84	15.68	0.03	8	9		86
SHAGAN	1985201	sha20jul85	5.90	4.06	3.90	0.06	15.84	15.64	0.10	9	5		74
SHAGAN	1987071	sha12mar87	5.40	3.81	3.67	0.05	15.63	15.49	0.05	8	13		11
SHAGAN	1987093	sha03apr87	6.20	4.48	4.39	0.05	16.33	16.15	0.07	23	6		140
SHAGAN	1987107	sha17apr87	6.00	4.05	3.68	0.12	15.81	15.56	0.06	6	19		86
SHAGAN	1987171	sha20jun87	6.10	4.01	3.95	0.04	15.82	15.72	0.05	17	4		107
SHAGAN	1987214	sha02aug87	5.90	3.86	3.78	0.03	15.64	15.52	0.07	17	6		72
SHAGAN	1987319	sha15nov87	6.00	4.45	4.39	0.02	16.21	16.17	0.03	23	3		103
SHAGAN	1987347	sha13dec87	6.10	4.28	4.11	0.07	15.98	15.84	0.05	16	8		137
SHAGAN	1987361	sha27dec87	6.10	4.13	3.99	0.08	15.84	15.72	0.03	13	8		117
SHAGAN	1988044	sha13feb88	6.10	4.19	4.10	0.04	15.96	15.89	0.04	15	9		125
SHAGAN	1988094	sha03apr88	6.00	4.30	4.20	0.03	16.05	15.87	0.08	13	7		135
SHAGAN	1988125	sha04may88	6.10	4.34	3.94	0.06	16.20	15.81	0.06	2	15		132
SHAGAN	1988258	shaganjve	6.10	4.28	4.21	0.03	16.09	16.03	0.03	23	3		108
SHAGAN	1988317	sha12nov88	5.26	2.78	2.70	0.03	15.20	14.91	0.06	2	17		15
SHAGAN	1988352	sha17dec88	5.67	4.11	4.01	0.07	15.98	15.87	0.05	18	6		68
SHAGAN	1989022	sha22jan89	5.95	4.26	4.17	0.02	16.05	15.94	0.05	17	4		118
SHAGAN	1989043	sha12feb89	5.71	4.30	4.19	0.05	16.12	15.87	0.09	15	4		63
SHAGAN	1989189	sha08jul89	5.48	3.87	3.78	0.04	15.63	15.51	0.04	17	6		22
SHAGAN	1989245	sha02sep89	4.98	3.46	3.31	0.05	15.32	15.17	0.03	10	10		6
SHAGAN	1989292	sha19oct89	5.74	4.28	4.17	0.05	16.17	16.00	0.08	15	4		70
SN_ZEMLYA	1973270	snz27sep73	5.83	3.68	3.69	0.12	15.55	15.44	0.05	5	1		
SN_ZEMLYA	1973300	snz27oct73	6.90	5.55	5.49	0.10	17.03	16.98	0.08	22	3		
SN_ZEMLYA	1974306	snz02nov74	6.75	5.27	5.25	0.06	16.75	16.73	0.08	21	1		
SN_ZEMLYA	1975291	snz18oct75	6.70	4.92	4.87	0.06	16.47	16.42	0.05	27	3		
USA	1967344	gasbuggy	5.10	3.68	3.61	0.05	15.61	15.55	0.10	4	0		29

Table 1

continued

Testsite	Date	Event Name	m_b	M_s Ave	M_s MLE	Stdev	Log M_0' Ave	Log M_0' MLE	Stdev	Nsig	Nnoise	Log M_i	Yield
USA	1968019	faultless	6.30	5.08	4.99	0.17	17.10	16.97	0.10	3	1		
USA	1969253	rulison	5.30	3.50	3.42	0.12	15.52	15.36	0.12	4	1		40
USA	1973137	rioblanco	5.40	3.61	3.51	0.14	15.68	15.60	0.06	5	1		100
USSR	1970346	sov12dec70	6.60	4.10	4.07	0.12	15.93	15.88	0.14	6	1		80
USSR	1970357	sov23dec70	6.60	4.20	4.23	0.10	16.00	15.95	0.14	6	0		75
USSR	1971082	sov23mar71	5.90	4.19	3.79	0.19	15.84	15.53	0.14	3	2		45
USSR	1976211	sov29jul76	5.90	3.91	3.85	0.09	15.44	15.33	0.04	6	0		58
YUCCA	1965337	corduroy	5.60	4.13	4.07	0.11	16.03	15.96	0.07	6	1		
YUCCA	1966139	dumont	5.80	4.18	4.05	0.07	16.15	15.98	0.08	9	5		
YUCCA	1967054	agile	5.80	4.29	4.05	0.05	15.89	15.77	0.02	2	1		
YUCCA	1967140	commodore	5.90	4.54	4.47	0.06	16.29	16.19	0.03	10	1	16.35	250
YUCCA	1967270	zaza	5.70	4.46	4.40	0.08	16.30	16.19	0.07	8	0		
YUCCA	1967291	lanpher	5.70	3.96	3.90	0.11	15.91	15.79	0.06	8	2		
YUCCA	1968250	noggin	5.60	4.17	4.02	0.10	16.02	15.90	0.07	10	2		
YUCCA	1969302	calabash	5.70	3.88	3.78	0.08	15.89	15.75	0.04	8	5	15.83	110
YUCCA	1970146	flask	5.60	3.72	3.59	0.10	15.74	15.58	0.06	10	5	15.55	105
YUCCA	1970287	tijeras	5.50	4.20	4.11	0.08	16.07	15.97	0.06	13	2		
YUCCA	1970351	carpetbag	5.70	4.36	4.13	0.06	16.10	15.93	0.06	6	7	16.13	220
YUCCA	1972265	oscuro	5.70	4.17	4.11	0.10	16.12	16.03	0.03	14	2		
YUCCA	1973116	starwort	5.60	3.87	3.78	0.06	15.78	15.65	0.08	6	1	15.62	90
YUCCA	1974191	escabosa	5.70	4.39	4.33	0.11	16.23	16.11	0.05	10	3		
YUCCA	1974242	portmanteau	5.80	3.95	3.78	0.07	16.06	15.75	0.08	4	3		
YUCCA	1975059	topgallant	5.70	3.76	3.65	0.08	15.99	15.71	0.07	4	6		
YUCCA	1975154	mizzen	5.70	4.07	3.97	0.11	16.05	15.96	0.05	12	6		
YUCCA	1975354	chiberta	5.70	4.15	4.09	0.06	16.11	16.03	0.08	3	0		
YUCCA	1976035	esrom	5.70	3.97	3.72	0.19	15.85	15.70	0.19	4	5		
YUCCA	1976035	keelson	5.80	4.12	4.01	0.08	16.15	16.02	0.05	5	4		
YUCCA	1976077	strait	5.80	4.41	4.30	0.07	16.23	16.11	0.07	9	2		
YUCCA	1977095	marsilly	5.60	3.76	3.59	0.18	15.77	15.55	0.05	7	8		
YUCCA	1977145	crewline	5.30	3.63	3.50	0.25	16.11	15.96	0.04	2	2		
YUCCA	1977231	scantling	5.60	4.17	4.04	0.07	16.07	15.96	0.04	12	6		

YUCCA	1977313	sandreef	5.70	4.41	4.28	0.08	16.26	16.16	0.06	17	2		
YUCCA	1977348	farallones	5.70	4.17	4.04	0.05	16.02	15.81	0.07	7	5		
YUCCA	1978054	reblochon	5.60	3.87	3.88	0.05	15.77	15.73	0.16	4	0		
YUCCA	1978082	iceberg	5.60	4.01	3.98	0.10	16.07	15.98	0.06	13	2		
YUCCA	1978193	lowball	5.50	4.02	3.95	0.08	15.84	15.74	0.04	16	3		
YUCCA	1978270	rummy	5.70	4.28	4.20	0.06	16.18	16.07	0.08	16	3		
YUCCA	1978322	quargel	5.10	4.07	3.74	0.08	15.60	15.20	0.11	2	4		
YUCCA	1979039	quinella	5.50	4.06	3.92	0.07	15.80	15.71	0.04	10	4		
YUCCA	1979249	hearts	5.80	4.26	4.19	0.07	16.13	16.02	0.05	16	4	16.16	140
YUCCA	1980107	pyramid	5.30	3.88	3.80	0.09	15.84	15.63	0.13	6	4		
YUCCA	1987169	brie		2.81	2.88	0.06	15.17	15.33	0.04	2	15		
YUCCA	1987197	midland	4.80	3.54	3.27	0.18	15.33	15.04	0.07	4	10		
YUCCA	1987197	midlandA		2.22	2.08	0.01	14.47	14.34	0.01	2	10		
YUCCA	1987225	tahoka	5.90	4.26	4.18	0.07	16.08	15.84	0.10	12	6		

Table 2

Surface-wave Magnitude/Yield Relations

Testsite	Number	M_s Ave	M_s MLE	Log M_0' Ave	Log M_0' MLE	Log M_i
ALL	98	2.10 ± 0.26	1.98 ± 0.27	13.91 ± 0.25	13.77 ± 0.25	14.05 ± 0.21 (43)
NTS	12	2.11 ± 0.21	2.02 ± 0.24	13.96 ± 0.17	13.82 ± 0.18	13.86 ± 0.24 (7)
AHAGGAR	2	2.55 ± 0.01	2.48 ± 0.06	14.41 ± 0.08	14.28 ± 0.02	
AMCHITKA	3	2.02 ± 0.03	1.92 ± 0.07	13.63 ± 0.08	13.53 ± 0.04	
CLIMAX	1	2.20	2.20	14.18	14.07	
PAHUTE	5	2.28 ± 0.11	2.21 ± 0.12	14.07 ± 0.14	13.92 ± 0.14	14.27 (1)
SHAGAN	74	2.09 ± 0.26	1.95 ± 0.27	13.90 ± 0.25	13.74 ± 0.25	14.08 ± 0.21 (36)
USA PNE	3	1.91 ± 0.30	1.83 ± 0.32	13.91 ± 24	13.81 ± 0.25	
USSR PNE	4	2.30 ± 0.17	2.18 ± 0.12	14.01 ± 0.23	13.87 ± 0.22	
YUCCA	6	1.95 ± 0.17	1.84 ± 0.19	13.84 ± 0.10	13.70 ± 0.12	13.79 ± 0.18 (6)

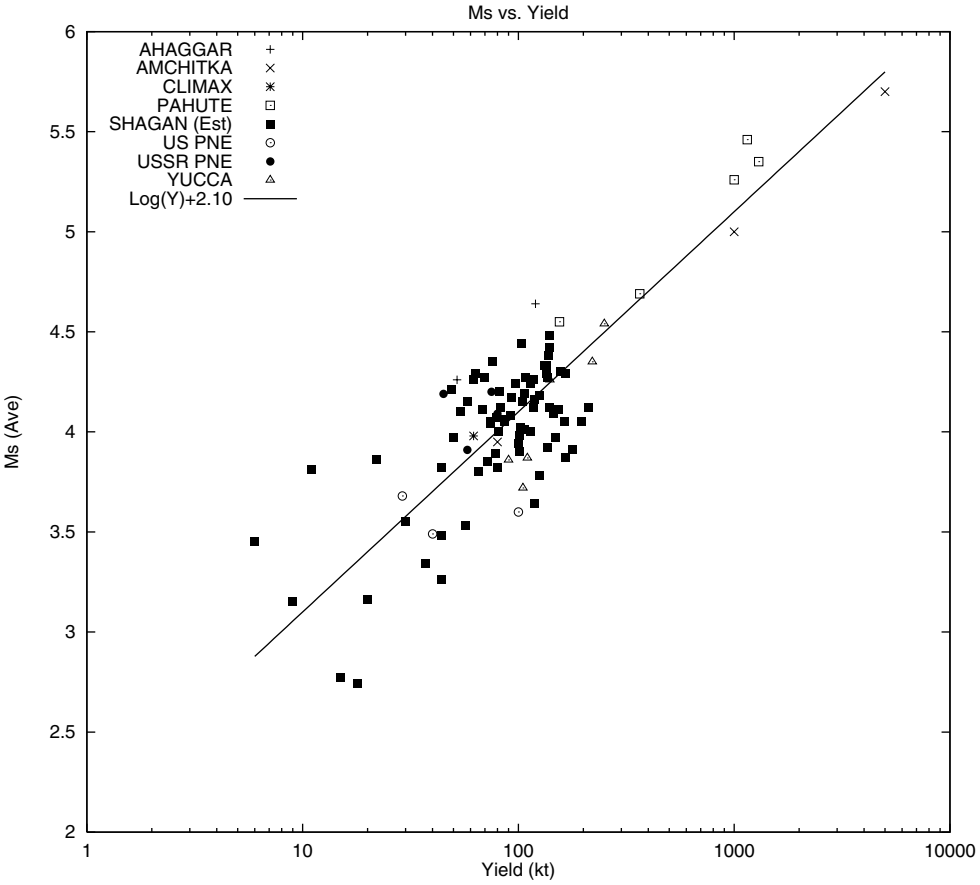

Figure 3
Network average M_s plotted vs. yield for the explosion data set of Table 1.

performed for a fixed depth and moment scales linearly with yield. These relations are compared to the scalar moments (path-corrected spectral magnitudes) estimates, and isotropic moments in Figures 9 and 10. The data have roughly the same magnitude and scatter as the different models, however the moment estimates are in general somewhat lower than the model predictions for hard rock.

Discussion and Conclusions

Table 2 and Figures 3–7 show magnitude/yield relations for five distinct surface-wave magnitude measures. Although there are small differences in scatter between the different magnitudes, all show a standard deviation in the observations of about 0.25 and none is dramatically better than any of the others. The magnitude yield relations for NTS and Shagan River are very close for time domain M_s and path-

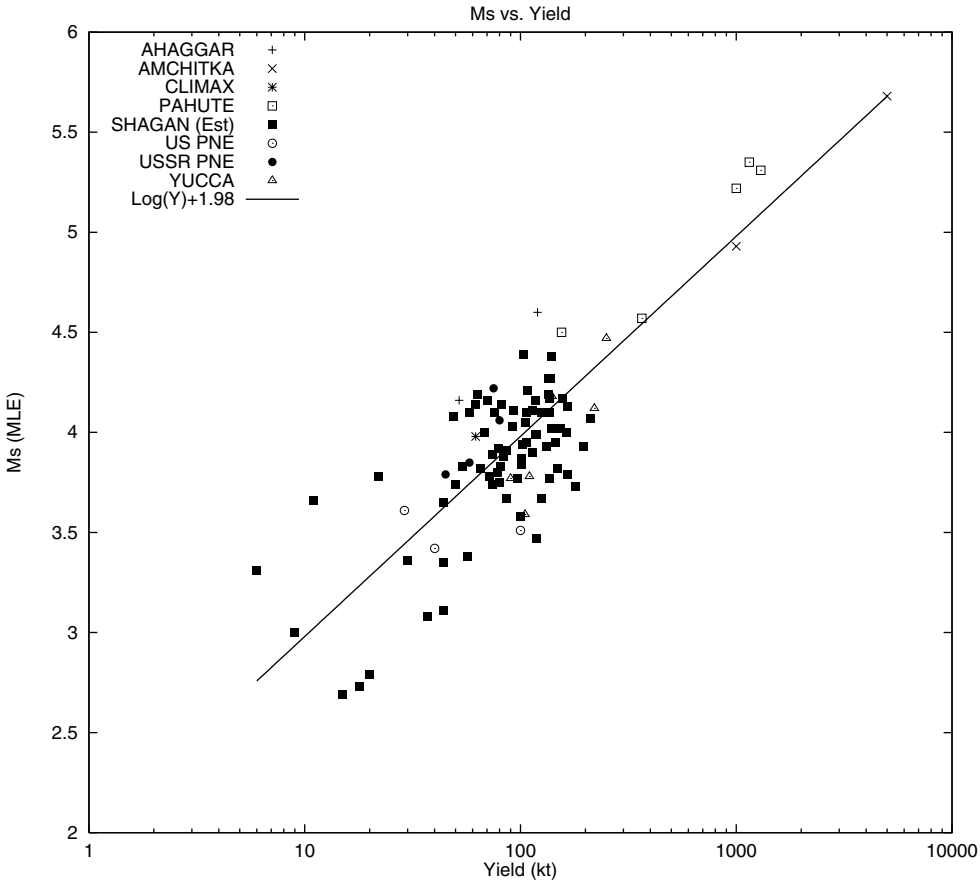

Figure 4
Maximum likelihood M_s plotted vs. yield for the explosion data set of Table 1.

corrected spectral magnitude M_0', however they differ by about 0.2 magnitude units for M_i as determined by moment-tensor inversion. This difference is a direct consequence of the assumption of different tectonic release mechanisms for the two test sites. It could be correct if the material properties for the two sites were very different, however as discussed by EKSTRÖM and RICHARDS (1994) it is likely that the assumption of pure thrust mechanism at Shagan River overcorrects the isotropic moment. A reasonable conclusion that can be drawn from this analysis is that yield estimates accurate to within a standard deviation of 0.25 in log yield can be estimated from surface-wave magnitudes or from moment-tensor inversion. However, the variability in surface waves due to tectonic release and other factors, and the inability to uniquely remove these effects is large enough that it is not possible to reliably make more accurate yield estimates using surface waves. Because the variability in surface-wave amplitude measurements is small, yield estimates can be made to this

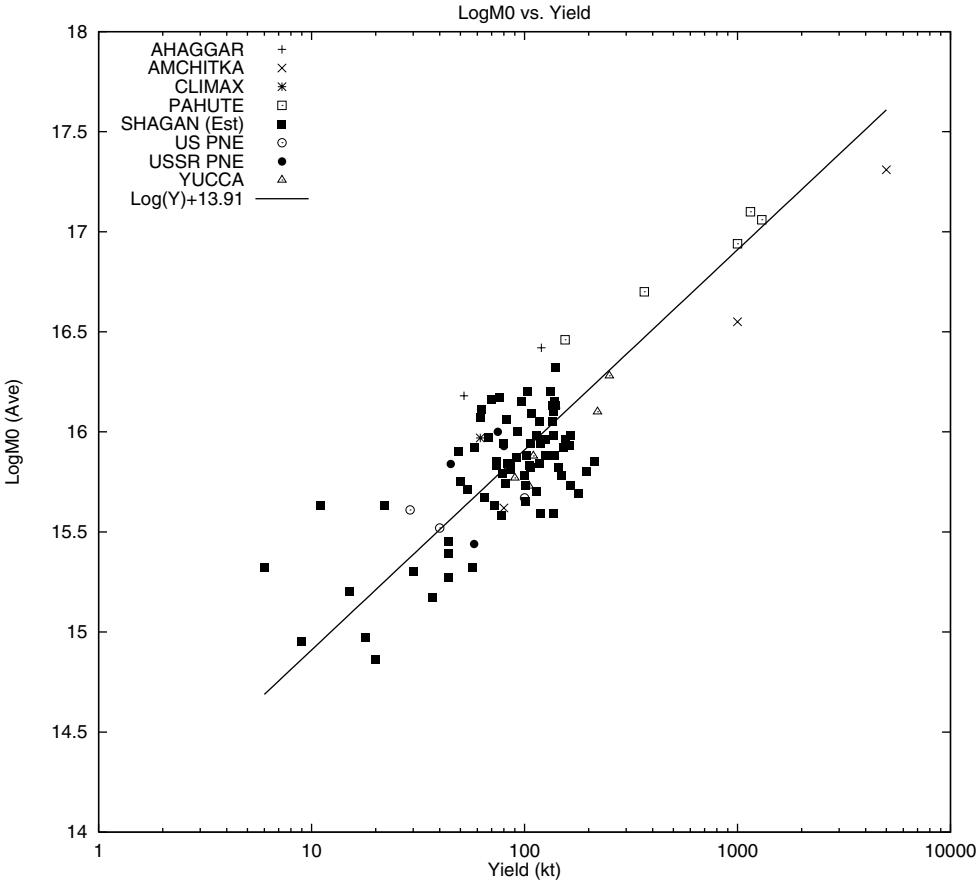

Figure 5
Network average path-corrected spectral magnitude Log M_0' plotted vs. yield for the explosion data set of Table 1.

accuracy from time domain or spectral magnitudes with a limited number of measurements. Moment-tensor inversion requires more measurements in order to solve for three independent quantities and because of uncertainties about the source mechanism does not significantly improve the accuracy of yield estimates.

Appendix A

Surface Wave Generation by a Moment Tensor Source

Surface waves are observed some distance from the source, often after having passed through a series of different earth structures. STEVENS and MCLAUGHLIN

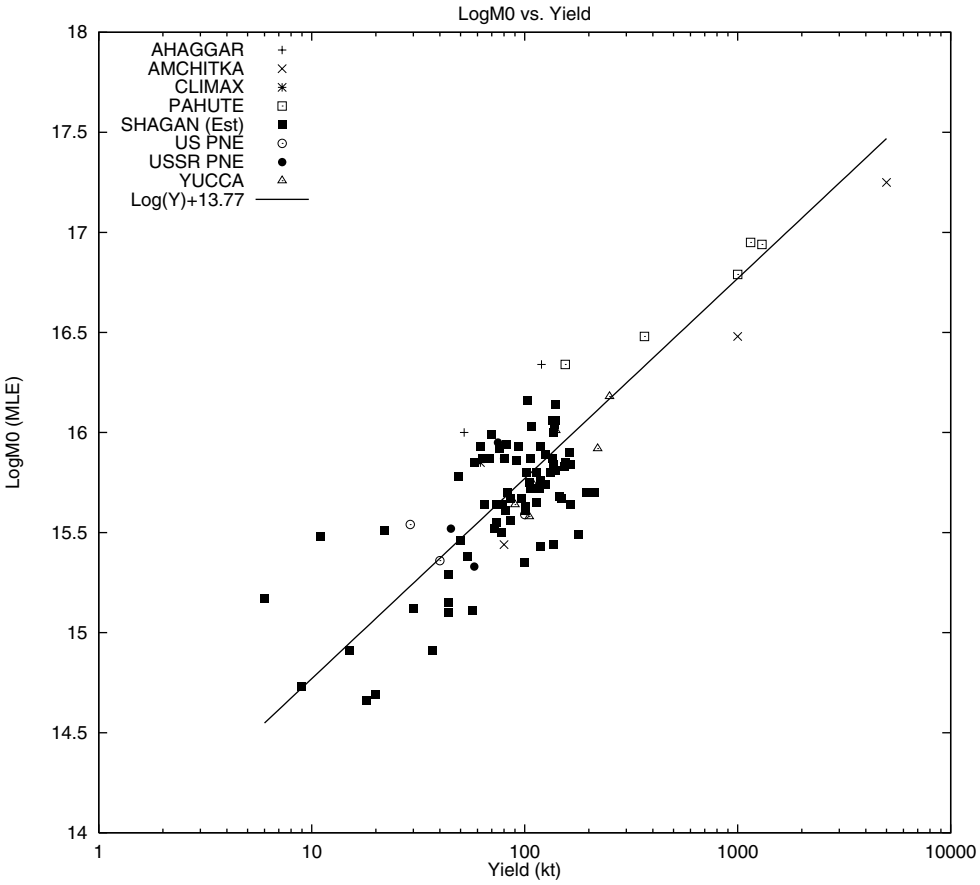

Figure 6
Maximum likelihood path corrected spectral magnitude Log M_0' plotted vs. yield for the explosion data set of Table 1.

(1999) show that the vertical displacement component of the Rayleigh wave, defined with vertical up, for a general source can be written in the form (notation follows HARKRIDER *et al.*, 1994):

$$u_z(\omega, r, \varphi) = \frac{1}{\sqrt{a_e \sin(r/a_e)}} \sqrt{\frac{2A_{R_1}}{\pi \omega c_1^2}} \sqrt{c_2 A_{R_2}} \times \exp\left[i\left(\pi/4 - \omega r/c_p - \gamma_p r\right)\right] F_s(\omega, \varphi, h) \quad \text{(A1)}$$

where ω is angular frequency, r is source to receiver distance, a_e is the radius of the earth, φ is azimuth, A_R is the Rayleigh wave excitation function, c is phase velocity, γ is the attenuation coefficient, and the subscripts 1, 2, and p refer to parameters

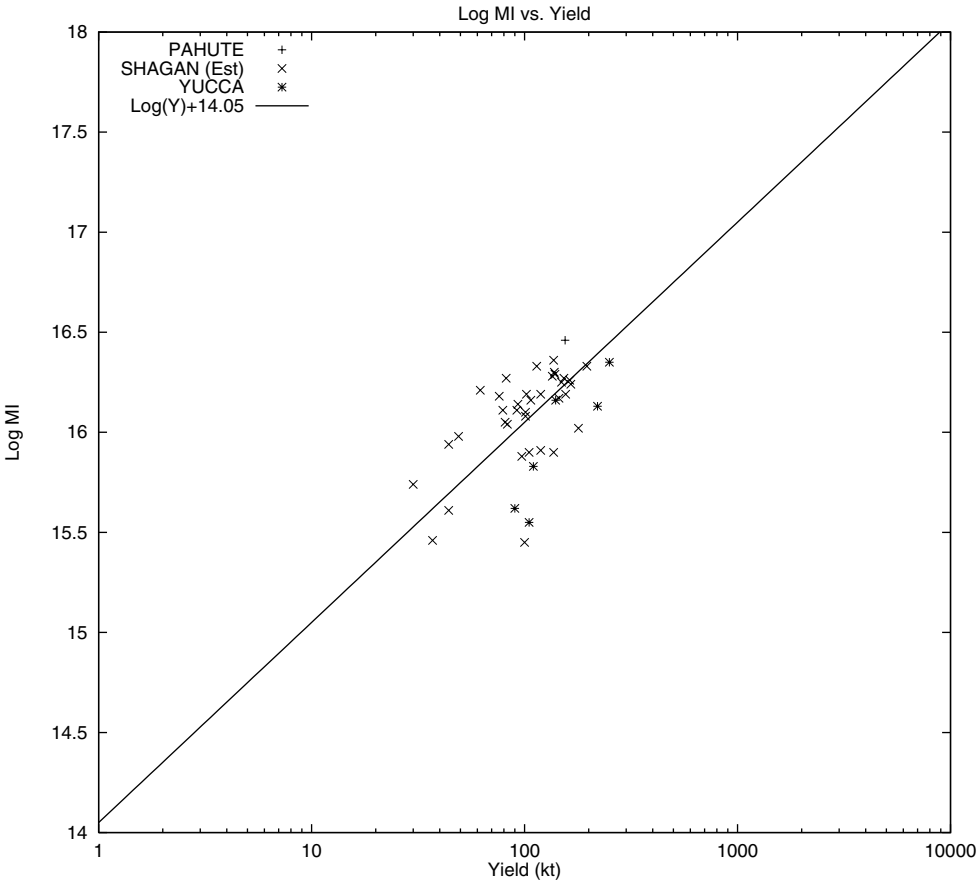

Figure 7
Isotropic moment M_i plotted vs. yield for the explosion data set of Table 1.

derived from the source-region structure, parameters derived from the receiver-region structure, and parameters which are defined by path averages, respectively. All source properties are contained in the function F_s which can be given in the form of moment-tensor components by:

$$F_s(\omega, \varphi, h) = \left[D\frac{\beta^2}{\alpha^2}\frac{M_{11} + M_{22} + M_{33}}{3} - B\frac{M_{11} + M_{22} - 2M_{33}}{12} \right] + \frac{iC}{2}[M_{13}\cos\varphi + M_{23}\sin\varphi] - \frac{A}{4}[(M_{11} - M_{22})\cos 2\varphi + 2M_{12}\sin 2\varphi] \tag{A2}$$

where

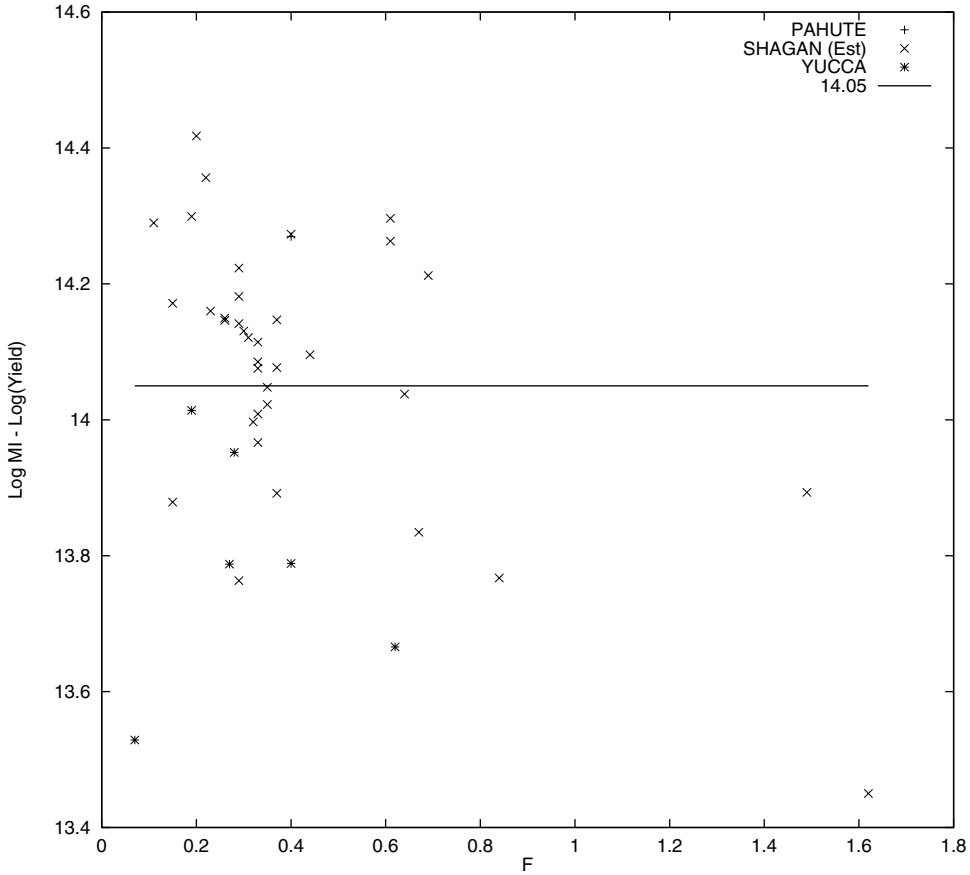

Figure 8
Difference between log moment and log yield shown as a function of the tectonic to isotropic moment ratio *F*.

$$A = -y_3(h)$$

$$B = -\left\{\left(3 - 4\frac{\beta^2}{\alpha^2}\right)y_3(h) + \frac{2}{\rho\alpha^2 k}y_2(h)\right\}$$

$$C = \frac{1}{\mu k}y_4(h)$$

$$D = y_3(h) - \frac{1}{2\mu k}y_2(h)$$

where y_1, y_2, y_3, y_4 are the vertical displacement, normal stress, horizontal displacement, and shear-stress eigenfunctions, respectively (TAKEUCHI and SAITO, 1972) and h is the source depth. Since the stress eigenfunctions both vanish for a free surface, for a shallow source, the coefficients reduce approximately to:

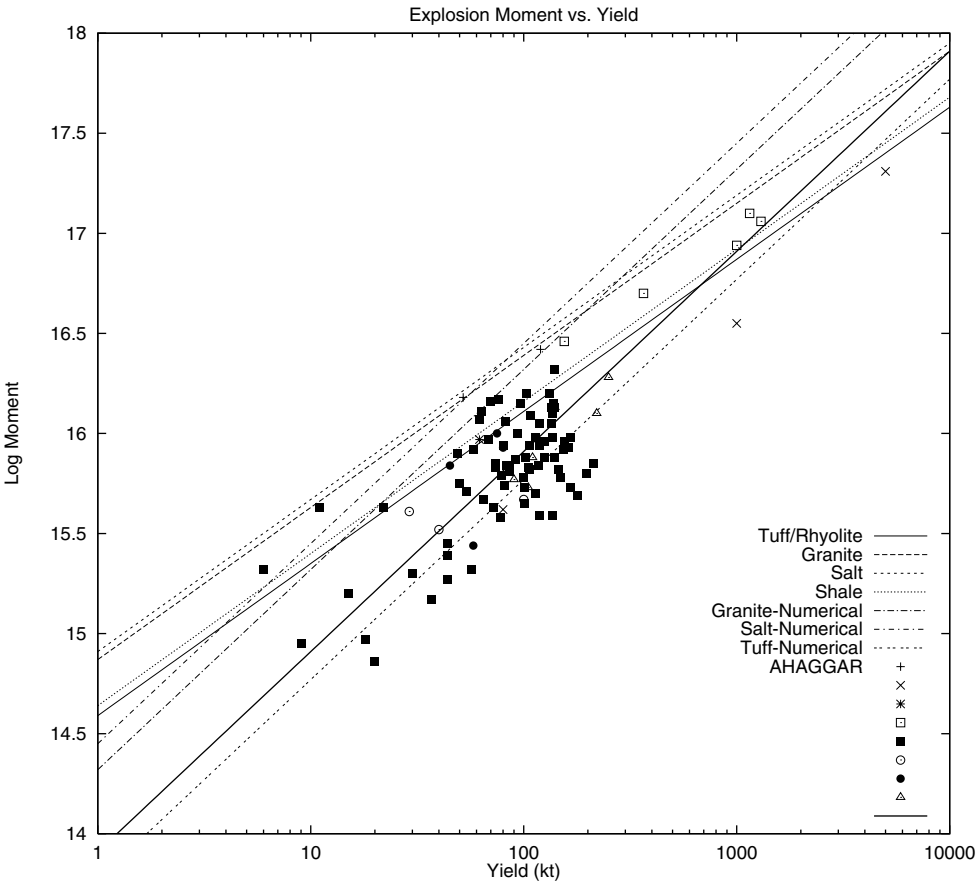

Figure 9
Log M_0' vs. yield curves for different material properties. Four of the curves are derived from the Mueller Murphy source models for tuff/rhyolite, granite, salt, and shale, and the other three from numerical models of explosions in tuff, granite and salt (STEVENS and DAY, 1985).

$$B \approx -\left(3 - 4\frac{\beta^2}{\alpha^2}\right) y_3(h)$$
$$C \approx 0$$
$$D \approx y_3(h) \quad .$$

Because C vanishes at the free surface, M_{13} and M_{23} do not contribute to surface-wave excitation for shallow sources at low frequencies, and conversely these moment-tensor components cannot be determined from surface-wave observations. The equations for Love waves can be written in a similar form to equation (A1). Love waves are also independent of M_{13} and M_{23} for shallow events, and are determined only by M_{12} and $M_{11}-M_{22}$. Moment-tensor inversion for a shallow source therefore

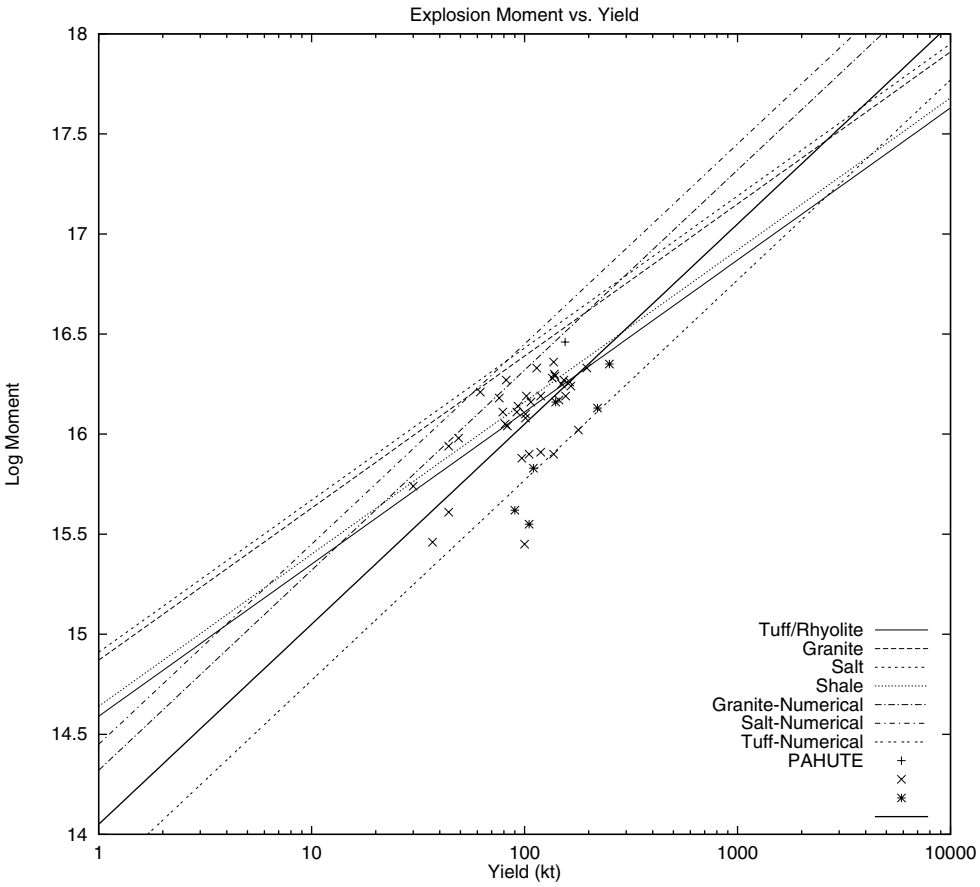

Figure 10
Log M_i vs. yield for different material properties. Models are the same as in Figure 6.

requires solving equation (A1) and the corresponding Love wave equation for the moment-tensor components M_{11}, M_{22}, M_{33}, and M_{12} using observations of Rayleigh and Love waves at multiple locations. Only three of the four parameters are independent, so moment-tensor inversion requires one additional constraint.

The isotropic moment is defined by $M_i = (M_{11} + M_{22} + M_{33})/3$. For an isotropic explosion source, the Rayleigh wave spectrum can be written:

$$u_z(\omega, h_x, r) = M_0' \frac{S_1^x(\omega, h_x) S_2(\omega) \exp[-\gamma_p(\omega) r + i(\varphi_0 - \omega r / c_p(\omega))]}{\sqrt{a_e \sin(r/a_e)}} \qquad \text{(A3)}$$

where φ_o is the initial phase equal to $-3\pi/4$,

$$S_1^x(\omega, h_x) = \sqrt{\frac{2A_{R_1}}{9\pi\omega c_1^2}}\left(\frac{1}{2\mu k}y_2(h_x) - y_3(h_x)\right) \ ,$$

$S_2(\omega) = \sqrt{c_2 A_{R_2}}$, and $M_0' = 3(\beta^2)/(\alpha^2)M_i$. M_0' is defined this way so that the source region excitation function is not explicitly dependent on local material properties at shallow source depths (STEVENS, 1986).

Acknowledgements

This work was supported by U. S. Air Force contract F19628-95-C-0110 and Defense Threat Reduction Agency contract DSWA01-98-C-0154.

REFERENCES

AKI, K., and TSAI, Y. (1972), *The Mechanism of Love Wave Excitation by Explosive sources*, J. Geophys. Res. *77*, 1452–1475.

ARCHAMBEAU, C. B. (1972), *The Theory of Stress Wave Radiation from Explosions in Prestressed Media*, Geophys. J. R. astr. Soc. *29*, 329–366.

BACHE, T. C. (1982), *Estimating the Yield of Underground Nuclear Explosions*, Bull. Seismol. Soc. Am. *72*, (6), part B, S131–S168.

DAY, S. M., RIMER, N., and CHERRY, J. T. (1983), *Surface Waves from Underground Explosions with Spall: Analysis of Elastic and Nonlinear Source Models*, Bull. Seismol. Soc. Am. *73*, 247–264.

DAY, S. M., CHERRY, J. T., RIMER, N., and STEVENS, J. L. (1987), *Nonlinear Model of Tectonic Release from Underground Explosions*, Bull. Seismol. Soc. Am. *77*, 996–1016.

DAY, S. M., and STEVENS, J. L. (1986), *An Explanation for Apparent Time Delays in Phase-reversed Rayleigh Waves from Underground Nuclear Explosions*, Geophys. Res. Lett. *13*, 1423–1425.

DEPARTMENT OF ENERGY (DOE) (1994), *United States Nuclear Tests, July 1945 through September 1992*, DOE Report DOE/NV-209, December.

EKSTRÖM, G., and RICHARDS, P. G. (1994), *Empirical Measurements of Tectonic Moment Release in Nuclear Explosions from Teleseismic Surface Waves and Body Waves*, Geophys. J. Int. *117*, 120–140.

GIVEN, J. W., and MELLMAN, G. R. (1986), *Estimating Explosion and Tectonic Release Source Parameters of Underground Nuclear Explosions from Rayleigh- and Love-wave Observations*, Sierra Geophysics Final Report to Air Force Geophysics Laboratory, Part 1, AFGL-TR-86-0171, SGI-R-86-126, July.

HARKRIDER, D. G., STEVENS, J. L., and ARCHAMBEAU, C. B. (1994), *Theoretical Rayleigh and Love Waves from an Explosion in Prestressed Source Regions*, Bull. Seismol. Soc. Am. *84* (5), 1410–1442.

HELLE, H. B., and RYGG, E. (1984), *Determination of Tectonic Release from Surface Waves Generated by Nuclear Explosions in Eastern Kazakhstan*, Bull. Seismol. Soc. Am. *74*, 1883–1898.

HERRIN, E., and GOFORTH, T. (1986), *Phase Analysis of Rayleigh Waves from the Shagan River Test Site in the USSR*, Bull. Seismol. Soc. Am. *76*, 1739–1754.

MARSHALL, P. D., SPRINGER, D. L., and RODEAN, H. C. (1979), *Magnitude Corrections for Attenuation in the Upper Mantle*, Geophys. J. *57*, 609–638.

MASSE, R. P. (1981), *Review of Seismic Source Models for Underground Nuclear Explosions*, Bull. Seismol. Soc. Am. *71*, 1249–1269.

MIKHAILOV, V. N. (1996), *USSR Nuclear Weapons Tests and Peaceful Nuclear Explosions*, Russian Federation for Atomic Energy report, ISBN 5-85165-062-1.

MUELLER, R. A., and MURPHY, J. R. (1971), *Seismic Characteristics of Underground Nuclear Detonations, I: Seismic Spectrum Scaling*, Bull. Seism. Soc. Am., *61*, 1675–1692.

MURPHY, J. R., and MUELLER, R. A. (1971), *Seismic Characteristics of Underground Nuclear Detonations, II: Elastic Energy and Magnitude Determinations*, Bull. Seism. Soc. Am., *61*, 693–1704.

MURPHY, J. R. (1977), *Seismic Source Functions and Magnitude Determinations for Underground Nuclear Detonations*, Bull. Seismol. Soc. Am. 135–158.

MURPHY, J. R. (1993), *Development of a Comprehensive Seismic Yield Estimation System for Underground Nuclear Explosions*, S-Cubed Final Report to Phillips Laboratory, SSS-DTR-93-13975, PL-TR-93-2157, May.

REZAPOUR, M., and PEARCE, R. G. (1998), *Bias in Surface-wave Magnitude M_s due to Inadequate Distance Corrections*, Bull. Seismol. Soc. Am. *88*, 43–61.

RINGDAL, F., MARSHALL, P. D., and ALEWINE, R. W. (1992), *Seismic Yield Determination of Soviet Underground Nuclear Explosions at the Shagan River Test Site*, Geophys. J. Int. *109*, 65–77.

RYGG, E. (1979), *Anomalous surface waves from underground explosions*, Bull. Seismol. Soc. Am. *69*, 1995–2002.

SALVADO, C., and MINSTER, J. B. (1980), *Slipping Interfaces: A Possible Source of S Radiation from Explosive Sources*, Bull. Seismol. Soc. Am. *70*, 659–670.

SATO, R. (1967), *Attenuation of Seismic Waves*, J. Phys. Earth *15*, 32–61.

STEVENS, J. L. (1982), *A Model for Tectonic Strain Release from Explosions in Complex Prestress Fields Applied to Seismic Waves from NTS and Eastern Kazakh Explosions*, Systems, Science and Software Technical Report, submitted to VELA Seismological Center, SSS-R-82-5358, January.

STEVENS, J. L., MCLAUGHLIN, K. L., SHKOLLER, B., and DAY, S. M. (1993), *2-D Axisymmetric Calculations of Surface Waves Generated by an Explosion in an Island, Mountain, and Sedimentary Basin*, Geophys. J. Internat. *114*, 548–560.

STEVENS, J. L., BARKER, T. G., DAY, S. M., MCLAUGHLIN, K. L., RIMER, N., and SHKOLLER, B. (1991), *Simulation of teleseismic body waves, regional seismograms, and Rayleigh wave phase shifts using two-dimensional nonlinear models of explosion sources*, In AGU Geophysical Monograph 65: *Explosion Source Phenomenology* (S. Taylor, H. Patton, P. Richards, eds.) ISBN 0-87590-031-3, pp. 239–252.

STEVENS, J. L. (1986), *Estimation of Scalar Moments from Explosion-generated Surface Waves*, Bull. Seismol. Soc. Am. *76*, 123–151.

STEVENS, J. L., and DAY, S. M. (1985), *The Physical Basis of the m_b:M_s and Variable Frequency Magnitude Methods for Earthquake/Explosion Discrimination*, J. Geophys. Res. *90*, 3009–3020.

STEVENS, J. L., and MCLAUGHLIN, K. L. (2001), *Optimization of Surface-wave Identification and Measurement*, Pure Appl. Geophys. *158*, 1547–1582.

TAKEUCHI, H., and SAITO, M. *Seismic surface waves*, In Methods of Computational Physics (B. A. Bolt, ed.), v. 11 (Academic Press, New York, 1972) pp. 217–295.

TOKSÖZ, N., and KEHRER, H. (1972), *Tectonic Strain Release by Explosions and its Effect on Discrimination*, Geophys. J. R. astr. Soc. *31*, 141–161.

VIECELLI, J. S. (1973), *Spallation and the Generation of Surface Waves by an Underground Explosion*, J. Geophys. Res. *78*, 2475–2487.

(Received August 6, 1999, revised July 28, 2000, accepted August 2, 2000)